Invited paper

# Grating out-coupled surface emitting high power semiconductor lasers

BOHDAN MROZIEWICZ*

Institute of Electron Technology, Warsaw, Poland

*Semiconductor lasers are capable of emitting high optical power if only their mirrors can withstand the flux of the optical energy they transmit. However, in the case of discrete broad-area edge emitting lasers the output beam is often divergent and multi-lobed. The monolithic resonant anti-waveguide arrays can be free of this flaw but their output power is still not very high and the fabrication process complicated and costly. The grating out-coupled surface emitting lasers seem to provide technically reasonable solution. Two types of such lasers: with linear and circular diffraction gratings, respectively, are discussed in this paper. In particular, principles of the design of monolithically integrated master oscillator power amplifier devices and recent advances in the circular diffraction surface emitting distributed Bragg reflector lasers, are described.*

## 1. Introduction

Semiconductor lasers are superior to other types of lasers in most of their properties including high external quantum efficiency (exceeding 80%), long operational lifetime (on the order of $10^5$ hours), small size and robustness. However, quality of the optical beam they emit is in general still a far cry to that inherent to gas and solid state lasers. Even if they generate in a single mode the output beam is usually strongly divergent due to a small aperture of the emitting spot, which in the case of the edge emitting lasers is in addition of a slit-like shape with dimensions of 0,1 μm × 5 μm to 100 μm. In result, the cross section of the beam emitted by such a laser is elliptical (Fig.1).

More circular beam crosssection can be accomplished by a special design of the heterostructure layers which leads to extension of the laser optical cavity in the transverse direction. It has been found, however, that at best the FWHM (full width half maximum) of the beam in that direction remains still larger than 8° [1]. Moreover, lasers with broad con-

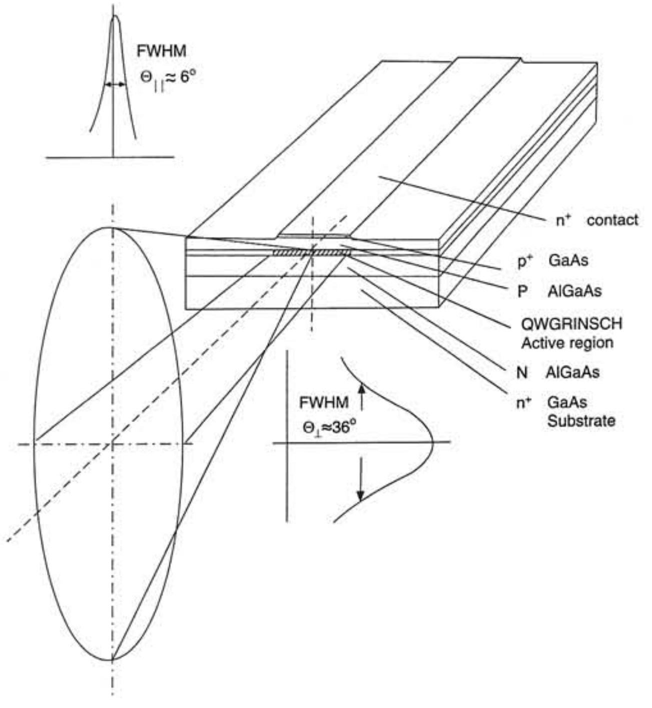


Fig.1. Schematic view of an edge emitting semiconductor laser and intensity distribution in its output light beam.

* Address for correspondence: Bohdan Mroziewicz, Institute of Electron Technology, Al. Lotnikow 32/46, 02-668 Warsaw, Poland

tacts designed for high power operation usually tend to generate many lateral modes what in general prohibits to obtain a diffraction limited beam [2].

Some solution to these problems may be sought in a monolithic array approach, in particular, if the arrays are of the resonant (ROW) type [3, 4, 5]. The latter can deliver continuos wave power of 0,5 W in a single lobe diffraction limited beam and peak-pulsed power of the order of 5–10 W in a near diffraction limited beam [6]. However, to execute high power single mode operation, the arrays must operate in a resonant out of phase leaky wave mode. For that purpose they must consist of a densely packed large number (e.g. 10) of index guided anti-waveguides [6, 7]. Practical ways of fabricating such arrays is by self-aligned process like in the case of complementary-self-aligned (CSA) arrays [8] or self-aligned-stripe (SAS) arrays [9, 10, 11]. Both types are quite complicated in design and expensive.

Another consideration that should be taken here also into account in the case of high power edge emitting lasers is the catastrophic optical damage of the laser mirrors (COMD). This damage occurs when density of the optical power in the beam emitted from the laser mirror exceeds some critical value and is caused by local overheating of the mirror surface because of the optical losses at this surface [12]. Due to small volume of the material that participates in the COMD process the latter takes place within the time shorter than 1 μs [13]. Therefore, in the case of drive current pulses longer than a few microseconds, a heat generated due to optical absorption spreads out because of the diffusion and some steady state is reached. The COMD threshold approaches then a CW limit and operation with current pulses wider than 1 μs is therefore termed "quasi-continuos" (q-CW). The COMD threshold is characteristic for particular semiconductor and depends on the wavelength generated in the laser [14]. The problem of COMD can be alleviated by coating laser mirrors with dielectric films (e.g. $Al_2O_3$) that protect their surface. This can increase the COMD threshold up to 4 times [14, 15]. Encouraging results have been obtained recently when coating the mirror with ZnSe layers [16]. Non-absorbing mirrors [17] and flared waveguide lasers [18] were another approaches devised towards solving the COMD problem but improvements did not justify high costs of these designs. Even the edge emitting coherent arrays are faced with the COMD limitations, since as for incoherent devices, maximum emitting apertures would be at most only 400-500 μm wide. Thus the projected maximum diffraction limited CW powers are in the 3-5 W range and

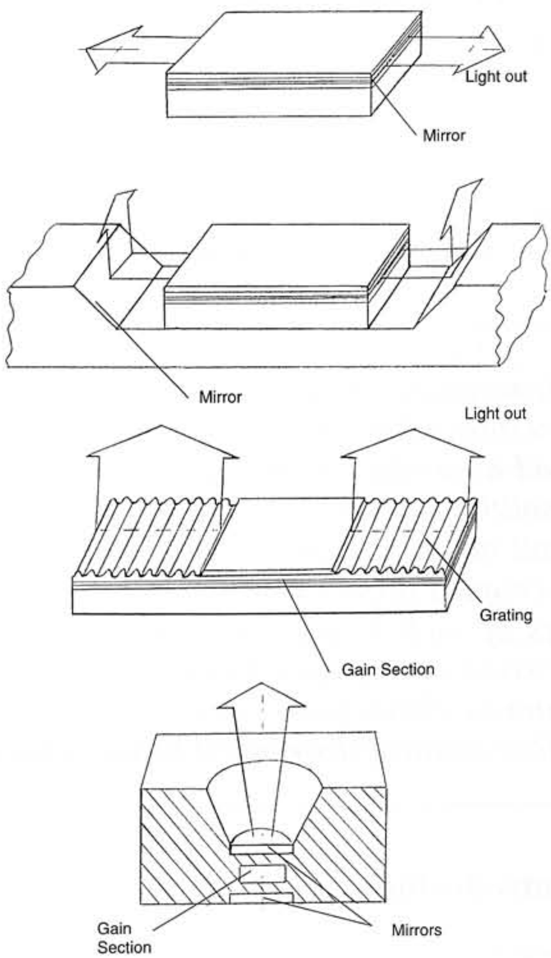


Fig.2. Schematic diagrams of surface emitting (SE) semiconductor lasers: a) integrated beam deflector SE laser, b) grating out coupled SE laser, c) vertical cavity SE laser (VCSEL).

beyond 5 W one will have to resort to 2D surface emitting arrays [19]. Heat generated in the laser due to nonradiative recombination and losses in the series resistance of the device is a second to the COMD limitation imposed on a semiconductor laser. This heat must be conducted away to a heat sink – a particularly serious problem in the case of CW operation. In order to solve this problem the laser chip must be firmly bonded to a heat spreader or heat sink on a large area of its base. Then adequate cooling systems have to be applied including those with microchannels [20, 21].

Thus we arrive to conclusion that the whole concept of the edge emitting lasers is inherently bounded by limitations imposed on the quality of the output beam. Most of those limitations would be removed if the output aperture of the laser were really enlarged. In quest for such laser design a notion of surface emitting lasers has been devised. Three classes of these lasers are presently known. These are integrated beam deflector surface-emitting lasers, grating out-coupled surface emitting lasers (GSE), and vertical cavity surface emitting lasers (VCSEL). Principle of construction of these lasers along with a conventional edge emitting laser is displayed in Fig. 2.

All surface emitting lasers have a potential advantage of large emitting spot that results in a low divergent beam but the grating out-coupled horizontal cavity lasers offer in addition effective heat sinking. This review will be devoted to grating out-coupled horizontal cavity lasers. Only AlGaAs/GaAs and InGaAs/GaAs material systems will be considered here as presently they are typically used for fabrication of high power lasers.

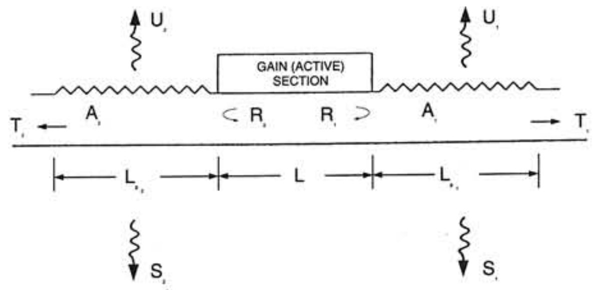


Fig.3. Schematic of the geometry of a horizontal cavity grating out-coupled surface emitting laser and the fractional powers reflected, radiated, transmitted, and absorbed [24].

## 2. Lasers with linear diffraction gratings

Bragg reflections from diffraction gratings having form of corrugations imprinted on a semiconductor surface have been exploited in a large family of DFB and DBR lasers [22]. Such corrugations reflect horizontally fraction of the propagating light and provide optical feedback if the Bragg condition $\lambda_B = \frac{m_B \Lambda}{2n_{eff}}$ is fulfilled. Here $\lambda_B$ is the resonant in-plane Bragg reflection wavelength for a grating period , $m_B$ = 1, 2, 3 is the Bragg reflection order, and $n_{eff}$ is the effective index of the guided mode. The feedback is therefore wavelength dependent which results in mode discrimination leading to a single mode operation [23].

Fraction of the light propagated in the laser cavity is out-coupled by the grating in direction different than horizontal. If the grating is the one of the second order, this direction is perpendicular to the optical cavity plane as it is illustrated schematically in Fig.3. Division of the light between horizontal and vertical directions is a function of the laser gain region structure and parameters of the grating. The various fractions of the incident power are denoted by **R=** reflected, **T=** transmitted, **U=** radiated into air, and **S=** radiated into substrate. The fractional power lost in the grating to optical absorption and scattering is given by:

$$\mathbf{A} = 1 - \mathbf{R} - \mathbf{T} - \mathbf{U} - \mathbf{S}$$

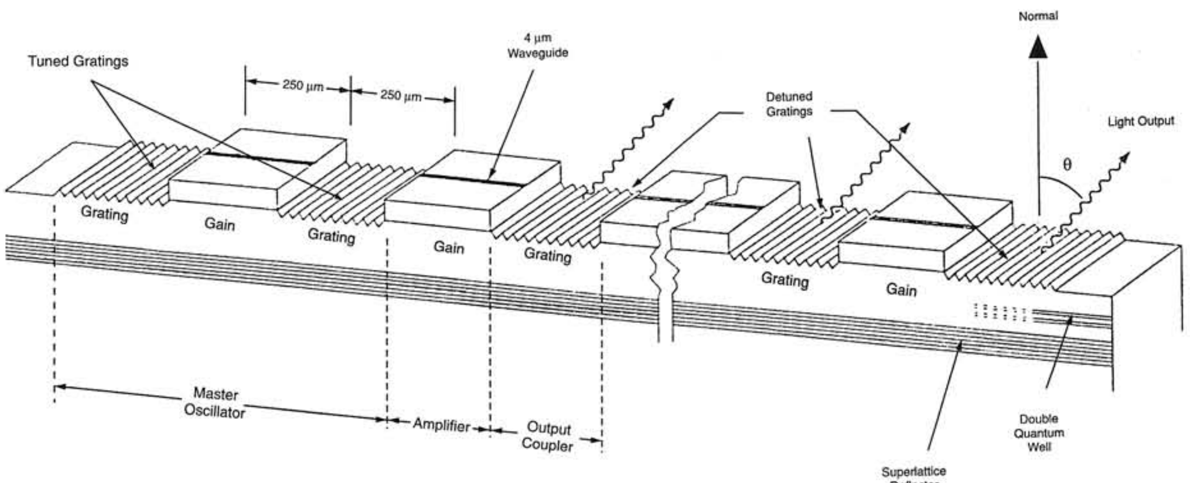


Fig.4. A monolithically integrated master-oscillator power amplifier. The signal from the master oscillator is amplified and injected into the detuned second-order-grating output coupler, which is designed to minimize reflections. This process is repeated to increase the coherent output from the amplifier array [26].

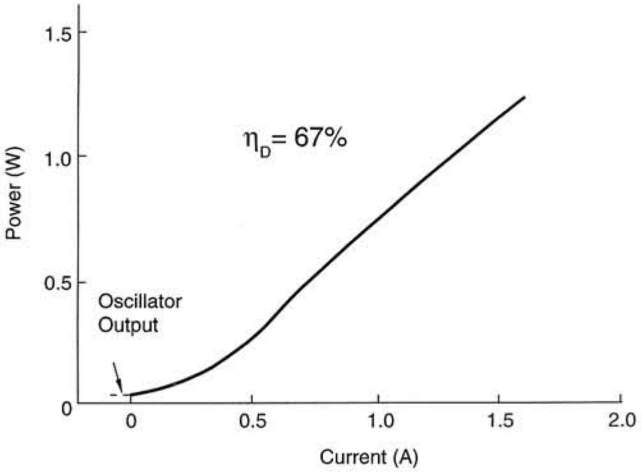


Fig.5. The light output as a function of the input current for a M-MOPA in which 9 amplifiers are driven in parallel. The spectral output at the maximum output power of 1.2 W replicates that of the master oscillator [26].

Detailed analysis of the device depicted in Fig. 3 is given in [24].

The output aperture of the lasers under consideration has the same dimensions as of the grating area and is large enough to secure very narrow output beam. Moreover, it can be easily noticed that the fraction of light propagating along the gain plane can be subsequently amplified by the next stage amplifier. This notion has lead to monolithically integrated master oscillator power amplifier M-MOPA i.e. the device shown in Fig.4 [25, 26]. It consists of a DBR master oscillator, preamplifier, out-coupling grating regions and amplifiers. The DBR oscillator is defined by second order gratings that are tuned to the peak of the gain and are approximately 150 μm long. Such length is a necessity if the grating is to inject a significant amount of power into the preamplifier and supply adequate feedback to the master oscillator. The signal is amplified in the preamplifier and injected into the first of a series of output couplers. The output couplers consist of second order gratings for which the Bragg condition is detuned from the gain peak of the injected signal to longer wavelengths. As a result, the reflectivity of the detuned second order grating is less than $10^{-5}$, whereas the output coupling can be as high as 85% for a 250 μm long grating region. Because of the very low reflectivities of the detuned grating output coupler, self oscillations do not limit the coherent output power of the M-MOPA. The output-coupled beam is radiated at an angle forward from the normal. A fraction of the light injected into the output coupler is transmitted to the next amplifier section, and the process of amplification and output coupling is repeated. An incremental 50 to 100 mW of coherent power results from each amplifier/output coupler pair. Light current characteristic of the M-MOPA displayed in Fig.4 is shown in Fig.5 [27]. This characteristic is exponential in the region where the modal power is below the saturation level of the amplifier and as the amplifiers reach saturation with increasing drive current it becomes linear up to the maximum output power of 1,2 W (under pulsed operation). Each additional amplifier/output coupler pairs adds greater than 100 mW of spectrally coherent output power.

One advantage of a M-MOPA design is that the spectral characteristics is a replica of the master oscillator, which is a single-mode narrow-line width source. Master-oscillator line widths have been measured as less than 1,5 MHz. No shift in the wavelength of the master oscillator takes place as the amplifiers are driven to higher output powers, indicating that the feedback from the amplifier sections is negligible and does not affect the operation of the master oscillator.

There is a great variety of designs of the M-MOPA lasers but all of them are based on the QW GRINSCH heterostructures. To secure single lateral mode operation of the device the DBR master oscillator has often

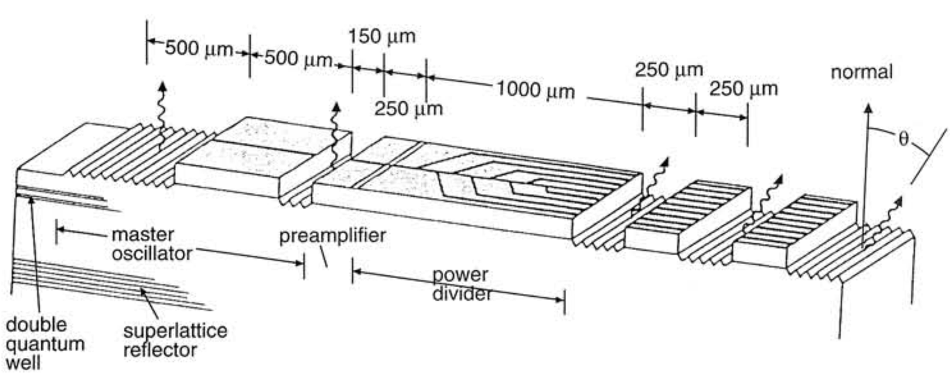


Fig.6. 2D monolithically integrated master oscillator power amplifier (2D M-MOPA). The amplifier stripes are spaced on 10 μm centres [28].

 

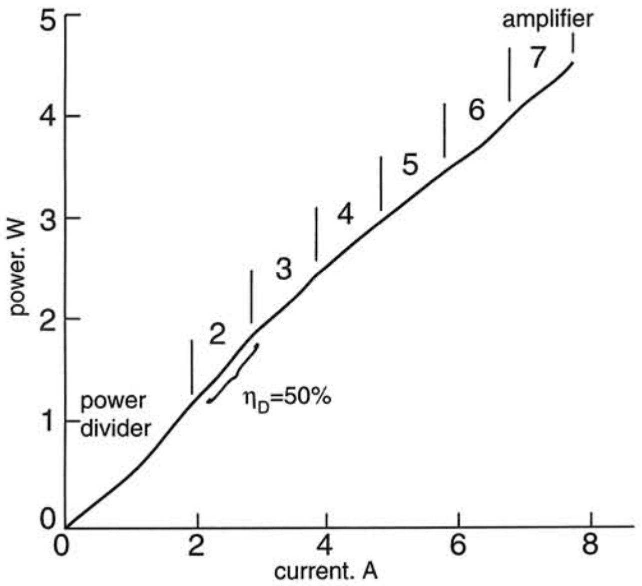


Fig.7. Output power versus current characteristic of a 4.5 W M-MOPA. The horizontal axis represents the total current of the amplifier chain. Each section on the characteristic indicates contribution of a particular section of the device. The output from the power divider and the first amplifier stage exceeds 1 W while each additional amplifier group adds approximately 550 mW of coherent output power [28].

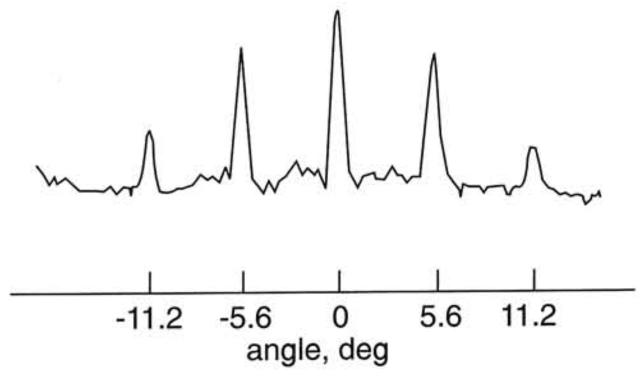


Fig.8. Far-field pattern of power divider in direction transverse to direction of propagation in a 9-stripe MOPA spaced on 10 μm centres [28].

an active region only 4 μm wide (see Fig.4). In that case the output beam is again asymmetrical in the crosssection. To avoid this feature and to increase the output power the M-MOPA design has been expanded to two dimensions by coupling the master oscillator to a branching wave guide network. The two-dimensional M-MOPA is presented in Fig.6. [28].

Its structure consists of seven power amplifier/output coupler stages, or a total of 63 radiating sources. As before the master oscillator consists of a DBR laser with second order gratings designed for feedback and transmission to the preamplifier. The amplified signal from the preamplifier is, however, distributed here alternatively by the power divider into nine parallel amplifier chains. The angle of the branching wave guide network is approximately 2° and is chosen to split approximately 10% of the power from the central amplifier chain at each split. Between each split the power in the central amplifier is amplified along the 250 μm length to maintain a nearly constant injected signal into each amplifier branch. The output of the power amplifier is injected into the detuned second order grating output coupler which out-couples more than 60% of the injected signal. The residual 40% portion of this signal is transmitted to the next power amplifier stage where it is again amplified and subsequently out-coupled. The 2D M-MOPA array was operated under pulsed conditions (pulse width 0.5 μs, repetition rate 1 kHz) and the total output power obtained from this device was 4.5 W at the peak differential efficiency 50% (Fig.7).

The spectral output of the power amplifier was identical to that of the master oscillator. Owing to the pitch of the output coupler grating, the emission was radiated at approximately 11° from the normal of the surface. The FWHM of the radiation pattern in the longitudinal direction was 0.25° which corresponds to the emission of a single 250 μm long emitter. The far-field pattern in the transverse direction is shown in Fig. 8.

The data represent the output of the power divider. It is important, that regardless of the mode discrimination and the different path lengths of the amplifier branches at low powers, emitters operated in an inphase mode. At high powers, however, the phase relationship of the discrete-output couplers of the original M-MOPA design are not fully correlated. In order to obtain a diffraction limited beam from the M-MOPA, the power-amplifier section can be redesigned to integrate the power amplifier with the output grating. The resulting design is a monolithically -integrated active grating MOPA (MAG-MOPA) [29]. This design uses a distributed amplifier/grating output coupler driven by a a single electrical contact, to continuously emit along a 5 mm aperture in a single diffraction-limited lobe (in the longitudinal direction). A schematic diagram of the MAG-MOPA with such distributed amplifier/grating output coupler is shown in Fig. 9.

The device consists of a conventional DBR master oscillator, a preamplifier, and a long current pumped detuned grating output coupler (active grating). The master oscillator and preamplifier are identical to those

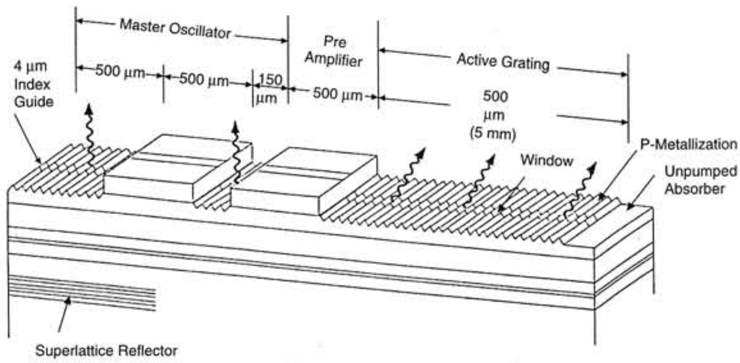


Fig.9. A monolithically integrated active-grating master oscillator power amplifier (MAG MOPA). Spatially coherent beam with a single diffraction lobe is generated due to continuos amplification and out-coupling [29].

in the M-MOPA (Fig.6). The active grating consists of a detuned output coupler that is integral to the gain region of the power amplifier, much like in a DFB laser, but with the grating pitch detuned from the gain peak to eliminate the reflective diffractive order. As a result, the propagating beam does not experience any phase distortion along the length of the amplifier and produces a diffraction-limited output beam. The guided-wave intensity within the active grating region grows from its injected value along the direction of propagation until the saturated local gain level decreases to the level of the guided mode losses. The losses include unsaturable absorption and scattering losses, in addition to the radiation losses which form the surface-coupled output. Once this equilibrium is reached, the guided wave intensity and the local carrier density remain constant along the remaining length of the aperture. The light/current curve of the MAG-MOPA was linear up to the highest powers measured (700 mW), with a differential slope efficiency of $\eta_D$= 15% and the maximum output power for a 5 mm long aperture was 1.3 W [26]. The bulk of the power was radiated from the active grating in a single diffraction-limited lobe at an angle of 10.2° forward of the normal. The FWHM of the amplifier emission was 0.012° which corresponded to the diffraction limit for the 5 mm long aperture. The radiation pattern in the transverse direction (perpendicular to the direction of propagation) exhibited a single Gaussian lobe with a FWHM of 9°, diffraction limited for the 4 μm wide lateral amplitude [29]. Consequently, the two-dimensional radiation pattern exhibited a single diffraction-limited lobe to the output power greater than 800 mW. It is reckoned that this technology is not limited by multi-mode oscillation but is scalable to output powers greater than 10 W CW [26].

Although the M-MOPA class lasers are complicated in structure and difficult to fabricate they have an advantage of being amenable to mass production in a planar process on large substrates and for the same reason suitable for monolithic integration with other photonic devices. They also offer several other advantages including highpower single spectral and spatial mode operation in a scalable geometry and a narrow spectral line width that is well behaved under modulation.

## 3. Circular diffraction gratings

Concept of the laser shown in Fig.4 can be quite obviously extended to a laser with circular diffraction gratings. The two possible designs for circular grating surface emitting DBR lasers are shown in Fig.10 [30].

In Fig.10a circular gain regions with different diameters are defined in the centre part of the device while the passive concentric circular gratings surround the gain section. Second-order circular gratings with appropriate width/period ratio are used to provide both the feedback for the resonance of circular modes and out-coupled radiation for surface emission. The advantage of this design is its simplicity of fabrication but it has the disadvantage of having an electrode in the centre part of the device. This problem can be eliminated by using the design of the Fig.10b.

In this design the second order gratings region with maximum surface radiation (width/period ratio of 1:2) is defined at the centre of the device. This region is surrounded by the circular gain section. Finally the

 

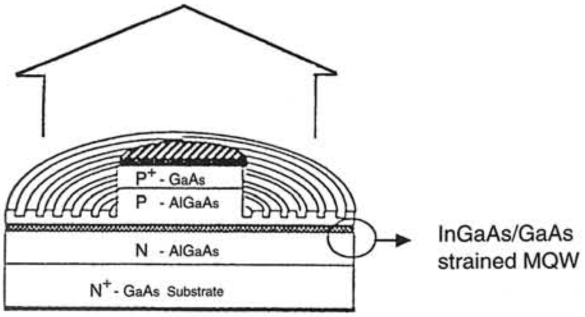


(a)

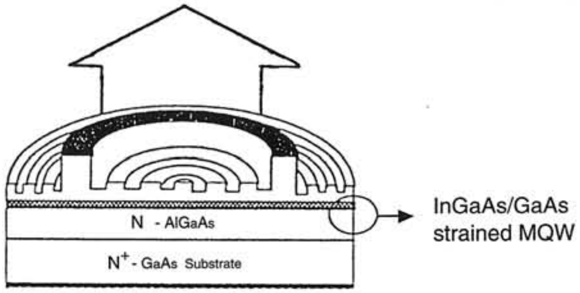


(b)

Fig.10. Two principle design configurations for CG SE DBR lasers; a) gain region is surrounded by a second order grating which provides both feedback and out coupling. b) central region accommodates a second order grating which serves as an out coupler. The gain region has a form of a ring which is surrounded by a first order circular grating that provides the feedback.

feedback for resonance is provided by a first order circular grating surrounding the gain section. The main advantage of such a design is in having the surface radiation emitted from the centre region of the laser and not being disturbed by the contact lead. The main difficulty with this design is the fabrication of high quality first order circular gratings which in the case of an InGaAs/GaAs structure and 0,98 μm wavelength have period of about 0,15 μm. Regardless of the design variant the laser gain region consists of QW GRINSCH heterostructure as in the case of MOPAs. Here the use of quantum wells for CG SE DBR laser structures is very convenient since the same structure can be used both for the active section to provide high differential gain and for the passive section as a low-loss wave guide. This we owe to low modal losses (below 10 $cm^{-1}$) in the MQW structures due to the step like density of states, band gap shrinkage effect and saturation of the excitonic absorption in these structures [31, 32]. As a result the whole laser structure can be grown in a single epitaxial process.

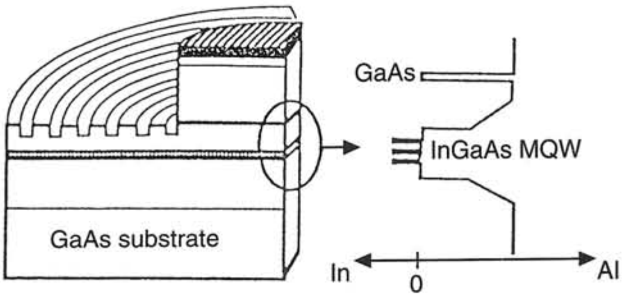


Fig.11. Schematic sectional view of a CG SE DBR laser of the type depicted in Fig.10a and with 60 μm diameter gain region [33].

Principle of a CG SE DBR laser with a second order grating designed for operation at 0.98 μm wavelength is shown in Fig.11 [33]. Thickness of the heterostructure layers in this device has been adjusted to obtain low threshold and high output power. A second order circular grating with a period of 239 nm and radial extent of 150 μm is surrounding the central gain region. Such gratings are usually written by electron-beam lithography in 0,25 μm thick polymethly metacrylate (PMMA) resist. They are subsequently transferred into the GaAlAs layer to a depth of about 0,15 μm by RIE (reactive ion etching). A thin layer of oxide is usually deposited on the grating section to protect the high aluminium concentration layer from being exposed to the air. Because of the two dimensional nature of the CG SE DBR lasers, the position control and uniformity of the circular gratings are the key factors. The addition of an etch stop layer in a strained multiquantum wells (MQW) structure is an efficient solution allowing both the use of the same structure for the active and passive sections and accurate positioning for the grating (see Fig.11).

The two most important parameters to be considered in the design of the described lasers are the power coupling efficiency ($C_0$) between the gain region and the grating region and the coupling coefficient (K) between the inward and outward propagating waves influencing the reflector coefficient ρ. These parameters have a significant impact on the threshold gain $g_{th}$ and consequently on the threshold current of the lasers as can be seen from the relation:

$$\Gamma g_{th} = \alpha_{\text{int}} + \left(\frac{2}{R}\ln\frac{1}{C_0\,\rho_0\,\rho_K}\right).$$

where $\alpha_{\text{int}}$ is the total internal loss, Γ is the optical confinement factor, R is the radius of the gain section,

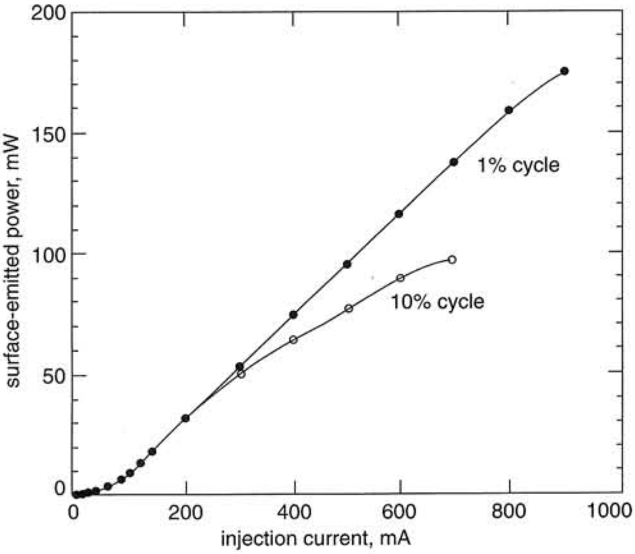


Fig.12. Output power versus drive current of the CG SE DBR laser shown in Fig.11. The gain region was of a diameter of 60 μm and the laser was driven with 1% and 10% (quasi-continuos) duty cycled pulses [33].

$\rho_0$ is the reflection coefficient at the centre (=1) and $\rho_K$ is the reflection coefficient at R.

In order to reduce the threshold current, high coupling efficiency and a high coupling coefficient are needed. The use of the same layer structure for the gain and grating sections is a simple approach to obtain high coupling efficiency. More detailed analysis of this relationship for CG SE DBR lasers can be found in [34].

The strength of the coupling coefficient depends on the grating order, grating profile, grating width and grating depth. Second order circular gratings with a rectangular profile and a valley/period ratio of 1:4 were considered. Such an aspect ratio provides strong reflectivity as well as surface radiation while minimizing the radiation into the substrate. A grating depth of over 0,1 μm was needed to obtain a high coupling coefficient [30]. The most critical steps in the fabrication of CG DBR lasers are the etch depth of the mesa which defines the gain section and the position of the top of the grating, the depth of the grating, and the most important one, the lithography of highly uniform circular gratings. The yield of the lasers strongly depends on how well these steps are controlled and in general, a significant effort is still needed to make these lasers manufacturable with high yield. Due to the small periodicity of the gratings, the CG SE DBR lasers have up to now been fabricated by electron beam or focused ion beam lithography [35, 36].

The threshold current measured for the laser as displayed in Fig.11 was 17 mA for both 1% and 10% duty cycles (Fig.12). This corresponds to a threshold current density of 600 A/cm$^2$ for the 60 m diameter circular gain sections. The external quantum efficiency was 14% and the output powers about 170 mW without saturation for 1% pulsed operation and about 97 mW for the quasi-continuos operation were obtained. The CW operation showed no change in the threshold current but the output power saturated at ~7,5 mW for 150 mA current. Single mode operation at low injection current and mode hopping at high injection were observed, nevertheless the far field divergence angle of 1,5° to 1,7° in all directions with a quasi circular crosssection was measured. At high power operation some of the lasers showed a multilobe far field pattern with a total divergence angle as high as 4,5° owing to the multimode operation of those lasers.

The design of a CG SE DBR laser configuration needs many further refinements. The structure should be soldered p-side down to improve heat sinking. Then the substrate must be transparent and a n-type contact of an appropriate geometry must be formed on the top of it. Multi-grating designs equivalent to M-MOPA lasers can be envisioned in which subsequent gratings would be separated by circular gain regions acting as amplifiers.

## 4. Conclusions

Surface emitting lasers show numerous advantages over high power edge emitting lasers. They are capable to generate high power narrow beams with a potential to operate in a single mode. They can be fabricated and tested on large substrates and thus will be strong contenders in the quest for high power medium price lasers. New generation of circular grating lasers look even more promising. Fabrication process of the circular gratings must be however improved, possibly by using holography methods. It is not unreasonable to expect that this design will overtake the lead in future developments.

## Acknowledgements

Part of this writing has been supported by the State Committee for Scientific Research under grant No 8 T11B 039 10.

## References

1. A. Malą g, B. Mroziewicz: *Vertical beam divergence of double barrier multiquantum well (DB*

 

*MQW) (AlGa)As heterostructure lasers.* J. Lightwave Technol. **14** (1996) 1514.
2. B. Mroziewicz: *Broad-area diode lasers with laterally controlled far-field pattern.* Electron Technol., **29** (1996) 15.
3. D. Botez, D.A. Ackley: *Phase-locked arrays of semiconductor diode lasers.* IEEE Circuits and Devices, **2** (1986) 8.
4. D. Botez, L.J. Mawst, G. Peterson, T.J. Roth: *Resonant optical transmission and coupling in phase-locked diode-laser arrays of antiguides: The resonant-optical-waveguide array.* Appl. Phys. Lett. **54** (1989) 2183.
5. D. Botez, L.J. Mawst: *Phase-Locked Laser Arrays Revisited,* IEEE Circuits and Devices **12** (1996) 25.
6. L.J. Mawst, D. Botez, T.J. Roth, G. Peterson, J. Rozenbergs: *CW high power diffraction-limited beam operation from resonant optical waveguide arrays of diode lasers.* Appl. Phys. Lett. **58** (1991) 22.
7. D. Botez, L.J. Mawst, G. Peterson: *Resonant leaky-wave coupling in linear arrays of antiguides.* Electron. Lett. **24** (1988) 1328.
8. D. Botez, L.J. Mawst, G. Peterson, T.J. Roth: *Phase-locked arrays of antiguides: Modal content and discrimination.* IEEE J. Quantum Electron. **QE-26** (1990) 482.
9. L.J. Mawst, D. Botez, C. Zmudzinski, M. Jansen, C. Tu, T.J. Roth, J. Yun: *Resonant self-aligned-stripe antiguided diode laser array.* Appl. Phys. Lett. **60** (1992) 668.
10. T.H. Shiau, S. Sun, C.F. Schaus, K. Zheng, G.R. Hadley: *Highly stable strained layer leaky-mode diode laser arrays.* IEEE Photonics Technol. Lett. **2** (1990) 534.
11. J.S. Major, Jr., D. Mehuys, D.F. Welch, D. Scifres: *High power high efficiency antiguide laser arrays.* Appl. Phys. Lett. **59** (1991) 2210.
12. W. Both, G. Erbert, A. Klehr, R. Rimpler, G. Stadermann, V. Zeimer: *Catastrophic optical damage in GaAlAsGaAs laser diodes.* IEE Proc. **134**. Pt.J. (1987) 95.
13. G. Harnagel, D. Welch, P. Cross, D. Scifres: *High power laser arrays: A progress report,* Lasers and Applications. **5** (1986) 135.
14. L.J. Mawst, A. Bhattacharya, J. Lopez, D. Botez: *8W continous wave front-facet power from broad-waveguide Al-free 980 nm diode lasers.* Appl. Phys. Lett. **69** (1996) 1532.
15. H. Brugger, P.W. Epperlein: *Mapping of local temperatures on mirrors of GaAs/AlGaAs laser diodes.* Appl. Phys. Lett. **56** (1990) 1049.
16. A.V. Syrbu, V.P. Yakovlev, G.I. Suruceanu, A.Z. Mereutza, L.J. Mawst, A. Bhattacharya, M. Nesmidal, J. Lopez, D. Botez: *ZnSe-facet-passivated InGaAs/InGaAsP/InGaP diode lasers of high CW power and "wall plug" efficiency.* Electron. Lett. **32** (1996) 352.
17. D. Botez, J.C. Conolly: *Nonabsorbing-mirror (NAM) CDH-LOC diode lasers.* Electron. Lett. **20** (1984) 530.
18. D.F. Welch, P.S. Cross, D.R. Scifres, W. Streifer, R.D. Burnham: *High power, AlGaAs buried heterostructure lasers with flared waveguides.* Appl. Phys. Lett. **50** (1987) 223.
19. L.J. Mawst, D. Botez, M. Jansen, C. C. Zmudzinski, S.S. Ou, M. Sergant, T.J. Roth, C. Tu, G. Peterson, J.J. Yang: *Two-dimensional surface-emitting leaky-wave coupled laser arrays.* IEEE J. Quantum Electron. **29** (1993) 1906.
20. D. Mundinger, R.Beach, W. Benett, R. Solarz, W. Krupke, R. Staver, D. Tuckerman: *Demonstration of high performance silicon microchannel heat exchangers laser diode array cooling.* Appl. Phys. Lett. **53** (1988) 1030.
21. L.J. Missaggia, J.N. Walpole, Z.L. Liau, R.J. Philips: *Microchannel heat sinks for two-dimensional high-power-density diode laser arrays.* IEEE J. Quantum Electron. **25** (1989) 1988.
22. B. Mroziewicz, M. Bugajski, W. Nakwaski: *Physics of Semiconductor Lasers.* (PWN, North-Holland, Amsterdam, Oxford, New York, Tokyo, 1991).
23. G. Morthier, P. Vankwikelberge: *Handbook of Distributed Feedback Laser Diodes.* (Artech House Books, Boston, London, 1997).
24. A. A. Hardy, D.F. Welch, W. Streifer: *Analysis of a Dual Grating-Type Surface Emitting Laser.* IEEE J. Quantum Electron. **26** (1990) 50.
25. D.F Welch, R. Waarts, D. Mehuys, R. Parke, D. Scifres, R. Craig, W. Streifer, High Power: *Diffraction-Limited, Monolithically Integrated Master Oscillator/Power Amplifier.* Appl. Phys. Lett. **57** (1990) 2054.
26. D.F.Welch: *Coherent lasers turn up the power,* IEEE Circuits and Devices **8** (1992) 17.
27. D. Mehuys, R. Parke, R.G. Waarts, D.F. Welch, A. Hardy, W. Streifer, D.R. Scifres: *Characteristics of Multi-Stage Monolithically Integrated Master Oscillator Power Amplifiers.* IEEE J. Quantum Electron. **27** (1991) 1574.
28. R. Parke, D.F. Welch, D. Mehuys: *Coherent operation of 2-D monolithically integrated master oscillator power amplifier* Electron. Lett. **27** (1991) 2097.

29. D.G. Mehuys, D.F. Welch, R. Parke, R.G. Waarts, A. Hardy, D. Scifres: *High Power Diffraction-Limited Emission from Monolithically Integrated Active Grating Master Oscillator Power Amplifier.* Electron. Lett. **27** (1991) 492.
30. M. Fallahi, F. Chatenoud, I.M. Templeton, M. Dion, Z. Wasilewski, M. Buchanan, R. Barber: *Recent Developments on InGaAs/GaAs Circular-grating Distributed Bragg Reflector Lasers.* Proc. SPIE, **2398** (1995) 135.
31. S. Tarucha, Y. Horikoshi, H. Okamoto: *Optical absorption characteristics of GaAs-AlGaAs multi-quantum-well heterostructure waveguides.* Jpn. J. Appl. Phys. **22** (1983) L482.
32. D.A. Miller, D.S. Chemla, D.J. Eilenberger, P.W. Smith, A.C. Gossard, W.T. Tsang: *Large room-temperature optical nonlinearity in GaAs-AlGaAs multiple quantum well structures.* Appl. Phys. Lett. **41** (1982) 679.
33. M. Fallahi, M. Dion, Z. Wasilewski, M. Buchanan, M. Nournia, J. Stapledon, R. Barber: *Performance improvement of circular-grating surface-emitting DBR lasers using an MQW structure with etch-stop laye*". Electron. Lett. **31** (1995) 1581.
34. C.M. Wu, T. Makino, S.J. Najafi, R. Maciejko, M. Svilans, J. Glinski, M. Fallahi: *Threshold Gain and Threshold Current Analysis of Circular Grating DFB and DBR Lasers.* J. Quantum Electron. **29** (993) 2596.
35. M. Fallahi, F. Chatenoud, I.M. Templeton, M. Dion, C.M. Wu, A. Delage, R.Barber: *Electrically pumped Circular Grating Surface-Emitting DBR Laser on InGaAs Strained Single-Quantum-Well-Structure.* IEEE Photon. Technol. Lett. **4** (1992) 1087.
36. M. Fallahi, M. Dion, F. Chatenoud, I.M. Templon, R. Barber: *High Temperature Operation of Circular-Grating Surface-Emitting DBR Lasers Fabricated on an InGaAs/GaAs structure.* IEEE Photonics Technol. Lett. **6** (1994) 326.

 